Proceedings of ERAD (2002): 200–205 © Copernicus GmbH 2002

ERAD 2002

Doppler radar observations of tropical cyclone Dina as it passed near La Réunion on 22 January 2002

F. Roux[1], **F. Chane-Ming**[2], **A. Lasserre-Bigorry**[3], **and O. Nuissier**[1]

[1]Laboratoire d'Aérologie (CNRS – Université Paul Sabatier), Toulouse, France
[2]Laboratoire de Physique de l'Atmosphère (Université de La Réunion), St-Denis, La Réunion, France
[3]Cellule de Recherche Cyclone (Météo-France), Ste-Clotilde, La Réunion, France

Abstract. Doppler radar observations of tropical cyclone Dina, as its eye passed at less than 100 km from the northern shores of La Réunion island (21°S, 55.5°W), are analyzed using the Ground-Based Extended Velocity Track Display (GB-EVTD) technique. The obtained results reveal the presence of strong swirling winds ($>$60 ms^{-1}) at 2 km altitude. A significant change in the location of the maximum winds in the low levels during the period of observations is probably related to the veering propagation of Dina and to the influence of the high topography of the island.

1 Introduction

Tropical cyclones (TCs) are threatening meteorological phenomena for islands and coastal regions in the Tropics. These perturbations are "warm-core" vortices where the strongest swirling winds occur in the lowest levels at some distance from the storm circulation center. In addition to wind damages, heavy rain cause floodings especially in mountainous regions, while high ocean tide and strong waves sweep the shores. Dedicated observations with instrumented aircraft, dropwindsondes, radar, satellites, as well as numerical models at various spatial resolution have provided valuable information on TCs. However, apart from geostationay satellite images, real-time data on TCs are relatively scarce and, even when the storm center is at relatively close distance ($\leq$100 km) from the threatened area, it is very difficult to estimate the wind intensity and its spatial distribution around the storm.

Ground-based Doppler radars are essential tools to observe mesoscale precipitating systems and, in addition to providing information on rain intensity, they can be of great help to estimate the wind structure of TCs. Lee et al. (1999, referred to as LJCD), Lee and Marks (2000) and Lee et al. (2000) have shown that, through the "Ground-based Velocity Track Display" (GB-VTD) technique, it is possible to deduce a plausible and physically consistent three-dimensional primary circulation of a landfalling TC using a single ground-based Doppler radar. However, the GB-VTD – derived wind description is not complete since only the symmetric part of the radial wind component can be obtained. In this paper, we show that the ground-based version of the extended VTD (EVTD, Roux and Marks, 1996) method – GB-EVTD – can alleviate this limitation.

The case study presented here concerns Doppler radar observations of tropical cyclone Dina near La Réunion island in the southwestern Indian ocean, on 22 January 2002. Section 2 summarizes the principles of GB-EVTD, Sect. 3 gives a brief summary of Dina's evolution and propagation from 16 till 26 January 2002, Sect. 4 presents the main results obtained from the GB-EVTD analysis of the Doppler data collected between 09:52 (all times UTC, local time is UTC+4) and 14:22, and some perspectives are discussed in Sect. 5.

2 The GB-EVTD analysis

The VTD and EVTD analyses (initially developed for airborne Doppler observations of TCs, Lee et al., 1994) consider a decomposition of the horizontal wind in the inner core region of TCs into circular harmonics supposing that (i) the air particles follow close streamlines around the storm center and, (ii) the lowest harmonics of the wind components are the most energetic ones. Within a ring of given width and depth at a radial distance ρ and an altitude z from the storm center at surface, tangential $\mathrm{V_T}$ and radial $\mathrm{V_R}$ wind components can be written as:

$$\begin{aligned} \mathrm{V_T} &= \mathrm{T_0} + \mathrm{T_1}\cos\Phi + \mathrm{T_2}\sin\Phi + \varepsilon_\mathrm{T}\,(\mathrm{n}\Phi, \mathrm{n} > 1) \\ \mathrm{V_R} &= \mathrm{R_0} + \mathrm{R_1}\cos\Phi + \mathrm{R_2}\sin\Phi + \varepsilon_\mathrm{R}\,(\mathrm{n}\Phi, \mathrm{n} > 1) \end{aligned} \quad (1)$$

Correspondence to: F. Roux (frank.roux@aero.obs-mip.fr)

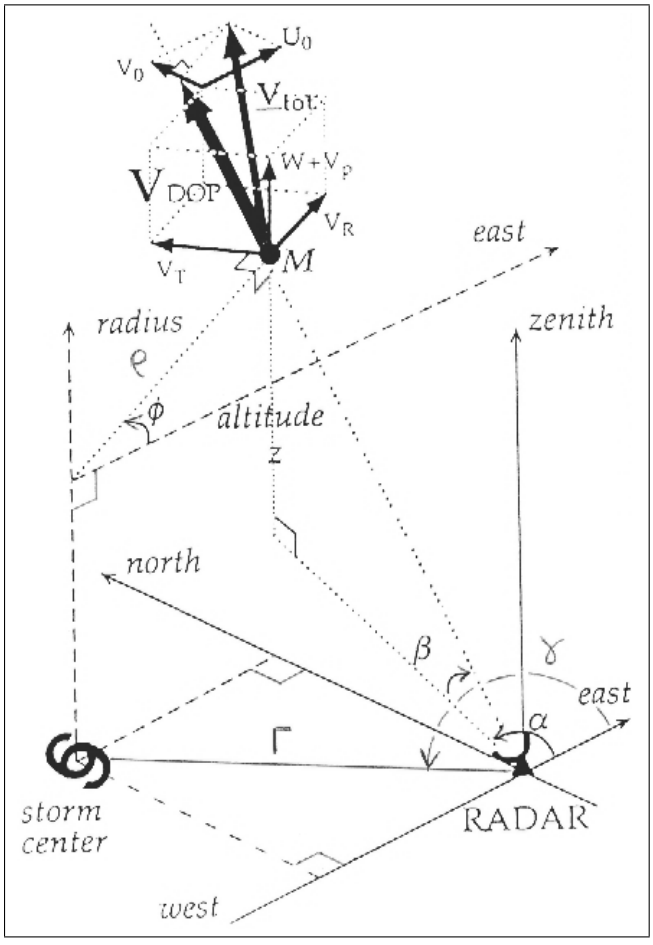

Fig. 1. Geometry of the GB-EVTD analysis.

where Φ is the azimuth relative to the storm circulation center (0 is eastward, Φ increases counterclockwise, see Fig. 1). ε_{T} and ε_{R} denote contributions from higher wavenumbers.

Once corrected for elevation β of the radar beam, hydrometeor fallspeed $\mathrm{V_p}$ which can be estimated from the radar reflectivity values (we use the same relations as Gamache et al., 1993), and storm motion (westerly $\mathrm{U_0}$ and southerly $\mathrm{V_0}$, determined from the successive positions of the storm center, see below), the Doppler radial velocity $\mathrm{V_{DOP}}$ measured in a TC with a ground-based radar can be written as:

$$\begin{aligned}\mathrm{V_{DOP}}^* &= \frac{1}{\cos\beta}\left(\mathrm{V_{DOP}} - \mathrm{V_p}\sin\beta\right) - \mathrm{U_0}\cos\alpha - \mathrm{V_0}\sin\alpha \\ &= \mathrm{V_T}\sin\left(\Phi-\alpha\right) + \mathrm{V_R}\cos\left(\Phi-\alpha\right)\mathrm{T_0}\sin\left(\Phi-\alpha\right) \\ &= \mathrm{T_0}\sin\left(\Phi-\alpha\right) + \mathrm{T_1}\cos\Phi\sin\left(\Phi-\alpha\right) + \mathrm{T_2} \\ &\quad \sin\Phi\sin\left(\Phi-\alpha\right)\mathrm{R_0}\cos\left(\Phi-\alpha\right) + \mathrm{R_1}\cos\Phi\cos \\ &\quad \left(\Phi-\alpha\right) + \mathrm{R_2}\sin\Phi\cos\left(\Phi-\alpha\right) \qquad (2)\end{aligned}$$

where α is the radar-relative azimuth (0 is eastward, α increases counterclockwise), β the elevation with respect to the horizontal. In the following, $\mathrm{V_{DOP}}^*$ will be simply referred to as $\mathrm{V_{DOP}}$. Hence, 6 unknown values ($\mathrm{T_i}$ and $\mathrm{R_i}$) have to be calculated for each ring at a given radius ρ from the storm center and at a given altitude z above mean sea level (MSL).

It can be deduced from LJCD that a modified Fourier analysis of the Doppler velocities in (2) as a function of Φ and d (the distance between the radar and the considered point) provides 5 independent values ($\mathrm{D_i}$):

$$\begin{aligned}\mathrm{V_{DOP}} &= \mathrm{D_0}\frac{\Gamma}{\mathrm{d}} + \mathrm{D_1}\left(\frac{\Gamma}{\mathrm{d}}\cos\Phi\right) + \mathrm{D_2}\left(\frac{\Gamma}{\mathrm{d}}\sin\Phi\right) \\ &\quad + \mathrm{D_3}\left(\frac{\Gamma}{\mathrm{d}}\cos 2\Phi\right) + \mathrm{D_4}\left(\frac{\Gamma}{\mathrm{d}}\sin 2\Phi\right) \quad \text{with :} \\ \mathrm{D_0} &= -\left(\frac{1}{2}\sin\gamma\right)\mathrm{T_1} + \left(\frac{1}{2}\cos\gamma\right)\mathrm{T_2} + \frac{\rho}{\Gamma}\mathrm{R_0} \\ &\quad + \left(\frac{1}{2}\cos\gamma\right)\mathrm{R_1} + \left(\frac{1}{2}\sin\gamma\right)\mathrm{R_2} \\ \mathrm{D_1} &= -\left(\sin\gamma\right)\mathrm{T_0} + \left(\cos\gamma\right)\mathrm{R_0} + \left(\frac{\rho}{\Gamma}\right)\mathrm{R_1} \qquad (3) \\ \mathrm{D_2} &= +\left(\cos\gamma\right)\mathrm{T_0} + \left(\sin\gamma\right)\mathrm{R_0} + \left(\frac{\rho}{\Gamma}\right)\mathrm{R_2} \\ \mathrm{D_3} &= -\left(\frac{1}{2}\sin\gamma\right)\mathrm{T_1} - \left(\frac{1}{2}\cos\gamma\right)\mathrm{T_2} + \left(\frac{1}{2}\cos\gamma\right)\mathrm{R_1} \\ &\quad - \left(\frac{1}{2}\sin\gamma\right)\mathrm{R_2} \\ \mathrm{D_4} &= +\left(\frac{1}{2}\cos\gamma\right)\mathrm{T_1} - \left(\frac{1}{2}\sin\gamma\right)\mathrm{T_2} + \left(\frac{1}{2}\sin\gamma\right)\mathrm{R_1} \\ &\quad + \left(\frac{1}{2}\cos\gamma\right)\mathrm{R_2}\end{aligned}$$

where Γ is the distance between the radar and the storm center, γ the angle between the East and the direction of the storm center as "viewed" from the radar (see Fig. 1). Since there are less available information (5 $\mathrm{D_i}$) than unknown values (3 $\mathrm{T_i}$ and 3 $\mathrm{R_i}$), some assumptions must be made to solve the problem. LJCD choose to neglect the wavenumber 1 component of the radial wind ($\mathrm{R_1}$ and $\mathrm{R_2}$). This leads to an overdetermined system of 5 equations with 4 unknowns ($\mathrm{T_0}$, $\mathrm{T_1}$, $\mathrm{T_2}$, $\mathrm{R_0}$) which can be solved in the least-square sense.

Our approach follows the same philosophy as EVTD (Roux and Marks, 1996): the availability of N successive radar sequences with different values of γ and Γ (resulting from TC motion) allows the 6 unknown values ($\mathrm{T_i}$ and $\mathrm{R_i}$) to be deduced from a series of N sets of ($\mathrm{D_i}$), i.e. N×5 equations (3). However, for this method to be efficient, two conflicting conditions must be satisfied:

(i) the values of γ and Γ must be as different as possible for the N sets of ($\mathrm{D_i}$) to be linearily independent, which favours large time intervals (or fast TC motion) between the successive radar scans,

(ii) this time interval must however be small (or storm evolution must be slow) so that the ($\mathrm{T_i}$ and $\mathrm{R_i}$) wind components do not vary too much during the series of radar scans.
Here, series of 2 or 3 radar scans separated by a maximum interval of 1 h have been considered, with differences of 5–10° in γ and 0–10 km in Γ.

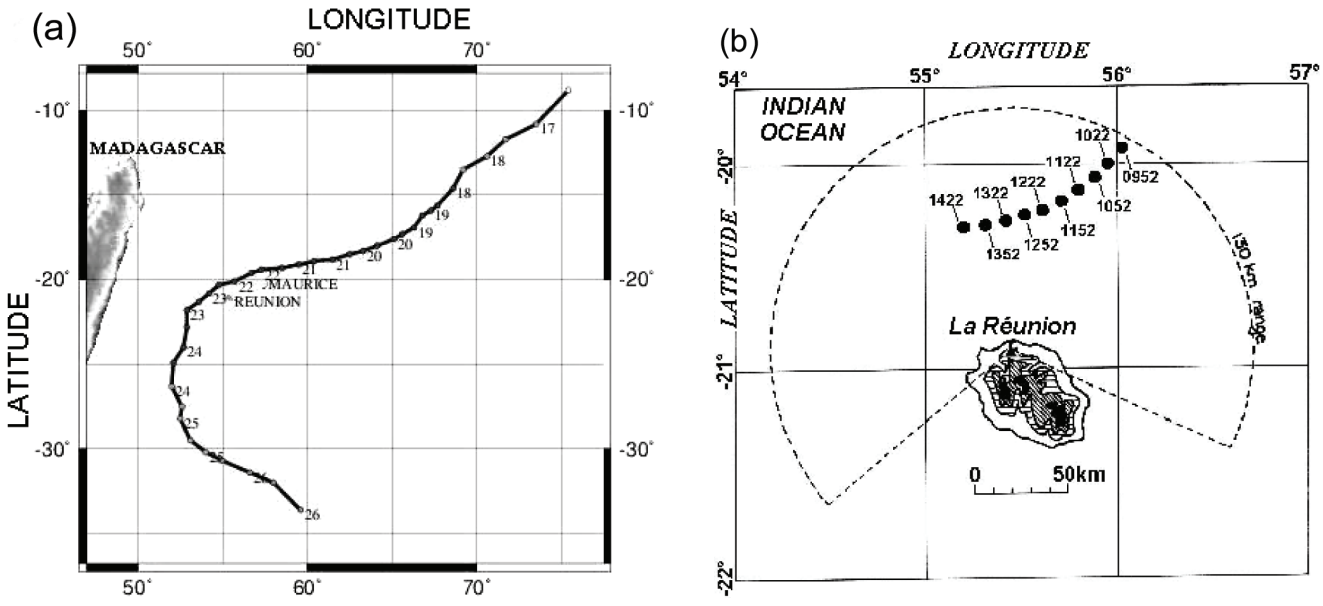

Fig. 2. (a) Trajectory of Dina in the southwestern Indian ocean from 17 till 26 January 2002 (from Météo-France), **(b)** location of Dina's center between 09:52 and 14:22 on 22 January. The dashed line contour is the limit of the Doppler scanning area with the radar close to the northern tip of La Réunion, shadings represent increasing altitudes (500, 1500 and 2500 m MSL).

3 Tropical cyclone Dina

Dina formed on 16 January 2002 from a large region of strong convection east of Diego Garcia island, near 76°W–8°S (Fig. 2a). On the 17th, it became a tropical depression, then a tropical storm while moving rapidly ($>10\,\mathrm{ms}^{-1}$) toward southwest. On the 18th, Dina was upgraded to tropical cyclone and it displayed a well-defined eye while its propagation speed slowed down to 6–7 ms^{-1}. It intensified on the 19th and during the morning of the 20th with estimated maximum winds of about 70 ms^{-1} and surface pressure of 910 hPa. During the afternoon of the 20th, the 21st and 22nd, surface wind and pressure varied from 60 to 65 ms^{-1} and from 910 to 920 hPa, respectively, while the direction of motion changed to west-southwestward.

Dina's eye went at closest distance ($<$130 km) from La Réunion on the 22nd between 10 and 18 UTC (Fig. 1b). Strong winds (40 to 70 ms^{-1}), heavy rain (500 to 1500 mm) and flooding, high swell (6 to 9 m) have caused major devastations in the northern half of the island. Dina was one of the strongest cyclone observed in La Réunion since 40 years, and the extent of the damages can also be explained by its relatively slow motion. The estimated cost is over 10 Millions of Euro and it will take months before the damaged infrastructure (roads, power and telephone lines, ...), industries, farms, buildings, houses, ... will be rebuilt.

Then, Dina's trajectory changed to southwards and its intensity decreased rapidly: 55 ms^{-1}/925 hPa on the 23rd at 00:00, 45 ms^{-1}/955 hPa on the 24th, 25 ms^{-1}/985 hPa on the 25th, after which it became strongly asymmetric and was carried along the westerly mid-latitude circulation as an extratropical depression.

4 Doppler radar observations

10 volumic scans at 130-km range have been conducted with the Météo-France operational Doppler radar located at 20.89°S, 55.42°W, 750 m MSL, every 30 min from 09:52 to 14:22 UTC on 22 January 2002 (Doppler data at 09:52 and 10:52 were corrupted). The radar antenna and radome were swept away by a strong wind gust at 14:50 and no data are available afterwards. As seen in Fig. 1b, due to the steep topography of La Réunion, with the highest peak – Pîton des Neiges – at 3069 m, radar data are unavailable in the southern quadrant (115–230° from north).

The storm center for each scan has first been determined as the geometric center of the eye region, characterized by low ($<$20 dBZ) reflectivity values. Although the so-determined propagation speed remained nearly constant (6.0 to 6.3 ms^{-1}, in agreement with the large-scale estimate), its direction changed substantially (from 33° to 90°) during the considered period. Such a situation has already been observed for tropical cyclones passing at a relatively close distance from La Réunion and is probably related to orographic influence.

GB-EVTD analyses were conducted with these Doppler data for 35 rings of 3 km width around the storm center ($0 < \rho < 105$ km) and 30 levels of 500 m depth ($0 < z < 15$ km). Three sets of scans were considered: 10:22–11:22 (intermediate time 10:52), 11:52–12:22–12:52 (intermediate time 12:22), 13:22–13:52–14:22 (intermediate time 13:52). First, it is to be noted that, due to the relatively high altitude of

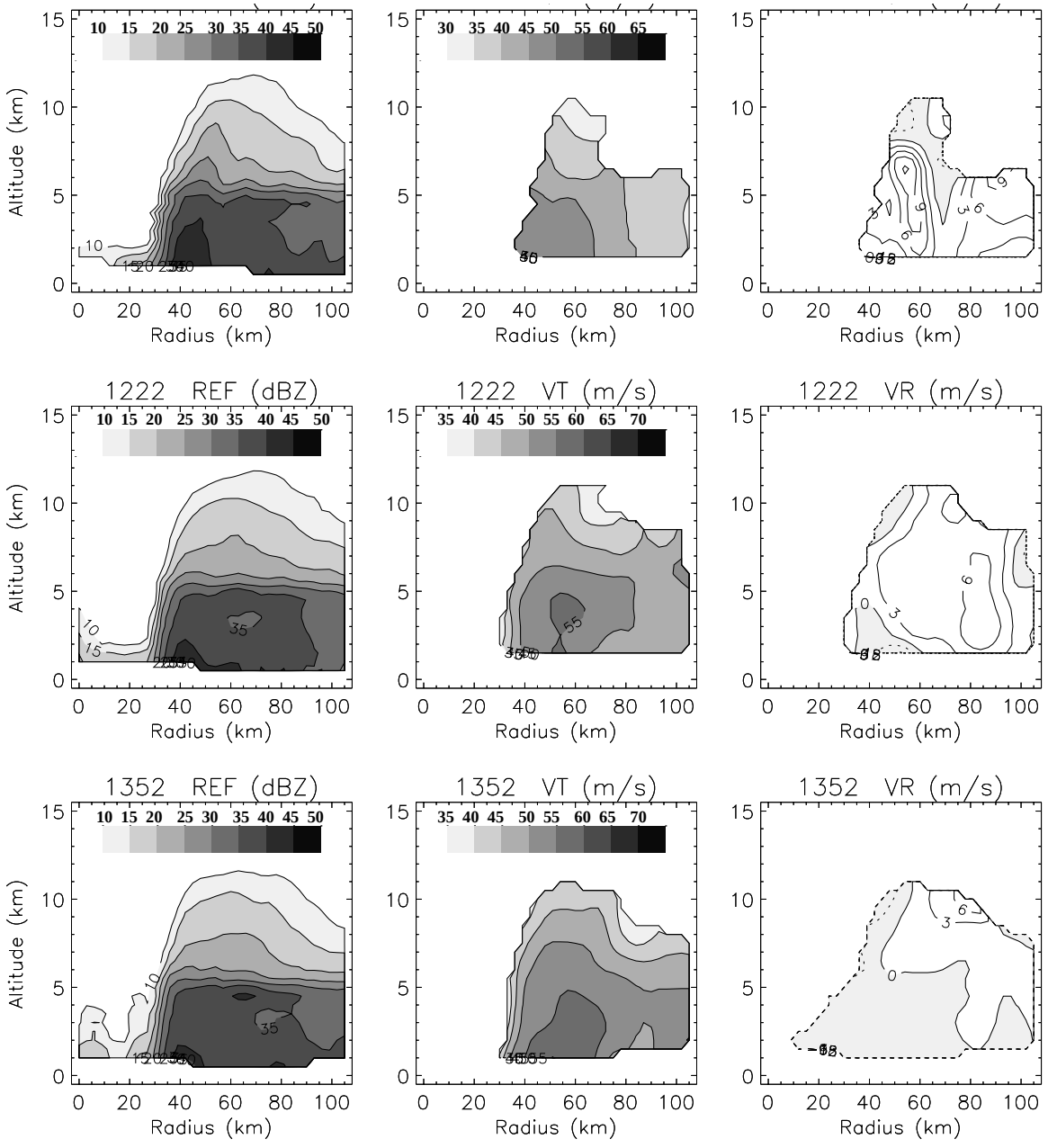

Fig. 3. Mean radial and vertical distribution of radar reflectivity (left column), tangential (middle column) and radial (right column) wind components for the composite analyses at 10:52 (upper row), 12:22 (middle row) and 13:52 (lower row). Steps for the contours are 6 dBZ for reflectivity, 6 ms^{-1} for tangential wind and 3 ms^{-1} for radial wind. Coordinate system is positive eastward and northward with its origin at the location of the radar (20.89°S, 55.42°E).

the radar and the 0.5° elevation of the first scan, the lowest level where GB-EVTD – derived values could be retrieved is 1.5 km. Also, GB-EVTD analysis could be conducted only for those rings where Doppler data were available within an azimuthal sector of more than 180°.

No GB-EVTD analysis was attempted for reflectivity since (i) this is a logarithmic quantity which cannot be added, and (ii) the negative values which could result from GB-EVTD analysis of reflectivity-derived precipitation contents (using the same relations as Gamache et al., 1993) would have no physical meaning. Hence, the mean radial and vertical distribution of reflectivity was derived from the azimuthal average of the estimated precipitation content (then retransformed in dBZ) for various radii and altitudes around the storm center. Since reflectivity data were not available throughout a 360° azimuthal sector for all the considered radii and altitudes, these mean values could differ slightly from true azimuthal means. The observed structure (Fig. 3, left column) is characteristic of an intense tropical cyclone with low values (<20 dBZ) in the eye at radii smaller than 30 km, strong

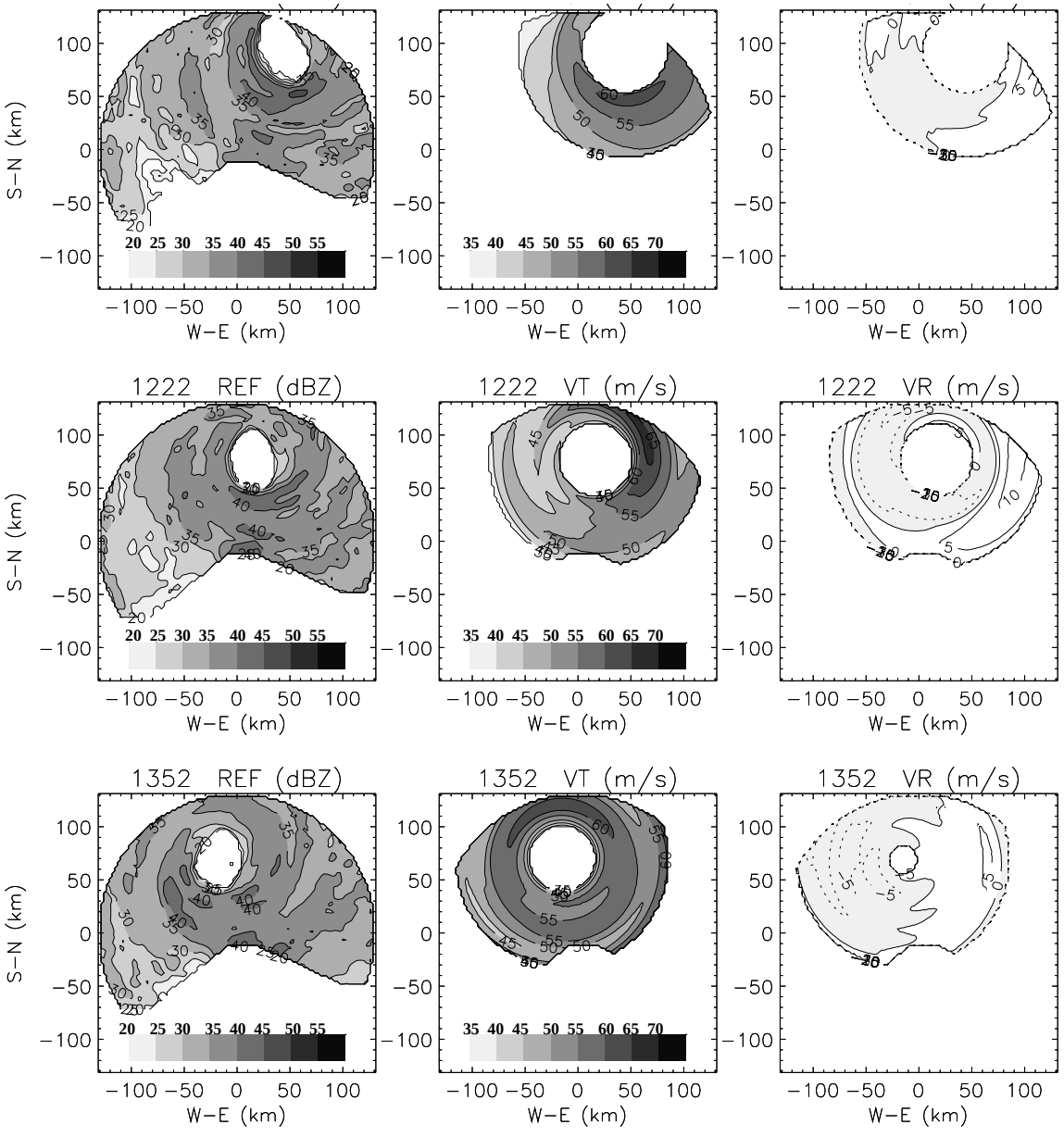

Fig. 4. As in Fig. 3, except for an horizontal cross-section at 2 km altitude.

(up to 40 dBZ) and elevated (6 dBZ limit up to 12–13 km altitude) ones in the eyewall region at radii between 30 and 80 km, slightly weaker and more stratiform values at radii larger than 80 km. The presence of low, but significant, reflectivity values in the eye could be an indication of a frictionnally forced vertical circulation below an eye inversion layer (Liu et al., 1999).

The mean circulation is deduced from the GB-EVTD – derived wavenumber-0 (symmetric) tangential T_0 (Fig. 3, middle column) and radial R_0 (Fig. 3, right column) wind components. The strongest tangential winds are found in the eyewall region, with maximum values larger than 55 ms^{-1}. Except in the eye (ρ <30 km), the mean tangential wind is everywhere larger than 35 ms^{-1} up to 11 km altitude. The mean radial wind was mostly outwards (up to +9 ms^{-1}), except at 13:52 with weak inflow (>-3 ms^{-1}). The main inflow feeding the inner core region of tropical cyclones is known to occur in the lowest levels (<1–2 km altitude, e.g. Liu et al., 1999) which were unfortunately inaccessible because of radar altitude and first-scan elevation.

Some changes occured with time. From 10:52 (upper row in Fig. 3) to 13:52 (lower row), the mean tangential wind increased substantially and a secondary maximum appeared in the outer part of the domain (ρ >100 km). Meanwhile, the main outflow region moved from the inner part of the domain ($50 < \rho < 60$ km) at 10:52, to the outer part ($70 < \rho < 90$ km) over the whole altitude range at 12:22, then in the upper part (z>8 km) at 13:52. Such an evolution

differs from the "eyewall replacement cycle" (Willoughby et al., 1982) during which reflectivity and tangential wind in an inner eyewall decrease while those in an outer eyewall intensify with associated changes in the outflow patterns. Here, there is no sign of a decrease of the radial distances of these eyewall regions as it is frequently observed in tropical cyclones undergoing such a cycle.

The horizontal distribution of radar reflectivity, tangential and radial winds at 2 km altitude is shown in Fig. 4. High reflectivity values ($>$40 dBZ) and strong tangential winds ($>$60–65 ms^{-1}) are found in the eyewall region. The estimated wind speed over La Réunion (near $(0, 0)$ in Fig. 4) is 54–58 ms^{-1} at 2 km altitude, which corroborates the observed values of 60–70 ms^{-1} at surface level. A notable feature is the changing location of the maximum winds: in the southern quadrant at 10:52, the eastern one at 12:22, the northern one at 13:52. This is correlated with slightly decreasing reflectivity values south of the eye and increasing ones at a larger radial distance, east and north of it. The radial wind shows a mean inflow from the west, with some indication of cyclonic (clockwise) turn with time. Such a pattern agrees with the southwestward to westward propagation of Dina (Fig. 2). In the upper levels (6–8 km altitude, not shown), distribution of radar reflectivity and tangential winds is more stationary, with maxima $>$25 dBZ and $>$50 ms^{-1} in the southern quadrant at 10:52, 12:22 and 13:52, while the main outflow is located to the northeast.

It is possible that the orographic influence of La Réunion island has slowed down the cyclonic circulation below 3 km altitude (that of the island highest peaks) in the southern part of the eyewall, and lead to intensification in its northern part. Such a change in the location of the maximum and minimum tangential wind would induce a torque which could explain the observed deflection of Dina's trajectory as it went close to La Réunion. Of course, additional studies are required to validate this hypothesis.

5 Conclusion and perspectives

The GB-EVTD analysis of data collected with an operational ground-based Doppler radar during the passage of a tropical cyclone at less than 130 km can provide useful information on its three-dimensaional tangential and radial wind structure (in addition to reflectivity). From such results, it is also possible to calculate the horizontal wind divergence and, through the integration of the air mass continuity equation, the vertical velocity. However, the lack of data in the lowest levels makes this attemps relatively difficult here. Availability of scans at 0° or negative elevation, especially for radars installed at elevated locations, would certainly alleviate this difficulty. Using the thermal wind relation, it is also possible to estimate the potential temperature perturbation, and surface pressure through the hydrostatic equilibrium.

A complementary approach is high-resolution ($<$2 km horizontally) numerical simulation. Nuissier et al. (2002) have shown that it is possible to initialize a non-hydrostatic nested model with a combination of operational large-scale analysis and a bogus vortex derived from Doppler radar observations. Such a technique will be used to study more precisely the structure and evolution of Dina on 22 January 2002. An interesting application will be the analysis of the interaction between the cyclonic circulation and the steep and relatively complex topography of La Réunion.

Acknowledgement. Partial fundings for this study have been provided by a INSU/PATOM grant. Thanks are due to MM. Mayoka and J. Quillet from Météo-France for their cooperation in providing the radar data.

References

Gamache, J.F., R.A. Houze Jr., and F.D. Marks Jr., 1993: Dual-aircraft investigation of the inner core of Hurricane Norbert. Part III : Water budget. J. Atmos. Sci., 50, 3221-3242.

Lee, W.-C., F.D. Marks Jr., and R.E. Carbone, 1994: A technique to extract real-time tropical cyclone circulation using a single airborne Doppler radar. J. Atmos. Oceanic Technol., 11, 337-356.

Lee, W.-C., B.J.-D. Jou, P.L. Chang, and S.-M. Deng, 1999: Tropical cyclone kinematic structure retrieved from single Doppler radar observations. Part I : Interpretation of Doppler velocity patterns and the GBVTD technique. Mon. Wea. Rev., 127, 2419-2439.

Lee, W.-C. and F.D. Marks Jr., 2000 : Tropical cyclone kinematic structure retrieved from single Doppler radar observations. Part II: The GBVTD-simplex center finding algorithm. Mon. Wea. Rev., 128, 1925-1936.

Lee, W.-C., B.J.-D. Jou, P.L. Chang, and F.D. Marks Jr., 2000: Tropical cyclone kinematic structure retrieved from single Doppler radar observations. Part III : Evolution and structures of Typhoon Alex (1987). Mon. Wea. Rev., 128, 3982-4001.

Liu, Y., D.-L. Zhang, and M.K. Yau, 1999: A multiscale numerical study of Hurricane Andrew (1992). Part II : Kinematics and inner core structure. Mon. Wea. Rev., 127, 2597-2616.

Nuissier, O., F. Roux, and R. Rogers, 2002: An intialization technique using airborne Doppler radar observations for numerical simulation of Hurricane Bret (21-23 August 1999). Proceedings 15th Hurr. Trop. Meteor. Conf., Amer. Meteor. Soc., San Diego (Ca., USA) , 403-404.

Roux, F. and F.D. Marks Jr., 1996: Extended velocity track display (EVTD): An improved processing method for Doppler radar observations of tropical cyclones. J. Atmos. Oceanic Technol., 13, 875-899.

Willoughby, H.E., J.A. Clos, and M.G. Shoreibah, 1982: Concentric eyewalls, secondary wind maxima, and the evolution of the hurricane vortex. J. Atmos. Sci., 39, 395-411.